


Cite this: *RSC Adv.*, 2021, 11, 19088

# Optimizing energy harvesting performance of silicone elastomers by molecular grafting of azobenzene to the macromolecular network

Min Gong,<sup>a</sup> Feilong Song,<sup>a</sup> Hejian Li,<sup>a</sup> Xiang Lin,<sup>a</sup> Jiaping Wang,<sup>b</sup> Liang Zhang<sup>\*a</sup> and Dongrui Wang<sup>id</sup><sup>\*a</sup>

The dielectric elastomer generator (DEG) has attracted significant attention in the past decade for harvesting energy from reciprocating mechanical motion owing to its variable capacitance under tension. However, the challenge of conceiving novel DEGs with high energy harvesting performance should be addressed. In this work, azobenzene molecules with strong polarity were synthesized and chemically grafted onto a hydroxyl-terminated polydimethylsiloxane (PDMS) network through a simple one-step process, offering a robust, molecularly homogenous silicone rubber. In addition, dimethyl silicone oil (DMSO) plasticizer was simultaneously added to reduce the mechanical modulus of the composite. The loading content of DMSO was firstly optimized in terms of the mechanical and dielectric properties of the resultant azo-*g*-PDMS/DMSO elastomers. Then, the effects of azobenzene loading on the morphology, and mechanical, dielectric and electric generation performances were thoroughly investigated. Overall, the dielectric permittivity displayed a rising trend with the increase of the azobenzene content while the breakdown strength increased initially and then decreased. The breakdown strength could reach as high as 73 V  $\mu\text{m}^{-1}$  by grafting with 7 phr of azobenzene while maintaining a relatively low mechanical modulus. Meanwhile, the as-prepared azo-*g*-PDMS/DMSO films exhibited enhanced energy harvesting density (0.69 mJ  $\text{cm}^{-3}$ ) and electromechanical conversion efficiency (5.01%) at a bias voltage of 1500 V, which were 2 and 2.5 times as much as those of the azobenzene-free matrix. This work provides ideas for future applications of DEG with high energy harvesting performance.

Received 22nd February 2021

Accepted 19th May 2021

DOI: 10.1039/d1ra01433a

rsc.li/rsc-advances

## 1. Introduction

With the rising concerns about global climate change and the energy crisis, developing renewable and environmentally friendly energy sources has been one of the most urgent challenges in modern society. Harvesting energy from the external environment is one of the most promising and effective strategies for sustainable development. So far, various energy harvesting systems capable of electromechanical transformation have been proposed and well-studied. Among them, dielectric elastomer generator (DEG) stands out owing to their favorable attributes of applicability to the time-varying nature of mechanical energy, high energy densities, independence of the operating frequency, and low-cost.<sup>1</sup> Virtually, DEG can be considered as a variable capacitor that consists of a soft/deformable dielectric elastomer film and two top and bottom compliant electrodes, forming into sandwich structures.<sup>2,3</sup> The

operation of DEG relies on the principle of electrostatic variable capacitance. Specifically, DEG is firstly stretched by external mechanical forces to increase the electrostatic potential energy of the charges present on the electrodes, followed by releasing to convert the elastic strain energy to the harvested electrical energy. The maximal electric energy ( $W_e$ ) generated by DEG for the polymer-based capacitors can be calculated through the following equation:

$$W_e = 0.5\varepsilon_0\varepsilon_rAdE_b^2$$

where  $\varepsilon_0$  and  $\varepsilon_r$  represent the vacuum permittivity and the relative permittivity, respectively,  $A$  and  $d$  represent the area and thickness of the dielectric,  $E_b$  represents the breakdown strength of the dielectric.

As indicated, the electric energy harvested by DEG is directly involved with the dielectric permittivity  $\varepsilon_r$  and breakdown strength  $E_b$ . Therefore, the output electric energy can be increased by developing a dielectric elastomer with higher dielectric permittivity for efficient energy transduction. Furthermore, high electric breakdown strength and low elastic modulus are also highly required to ensure higher operating

<sup>a</sup>School of Chemistry and Biological Engineering, University of Science & Technology Beijing, Beijing, 100083, PR China. E-mail: zhangliang@ustb.edu.cn; wangdr@ustb.edu.cn

<sup>b</sup>China Astronaut Research and Training Center, Beijing 100094, PR China



voltage tolerance and high mechanical energy storage. All these essential factors should be comprehensively considered while conceiving novel DEG with improved electromechanical transformation performances.

Up to now, commonly used dielectric materials are mainly relating to acrylic elastomers (*e.g.*, commercial adhesive tape VHB by 3M), natural or synthetic (*e.g.*, styrene-based) rubber, and silicone elastomer. Among all these candidates, silicone rubbers, in particular polydimethylsiloxane (PDMS), have been regarded as the most promising for future DEG applications because of the relatively low elastic modulus, thermal stability, biocompatibility, good applicability to different manufacturing techniques, and feasibility of physicochemical modification.<sup>4,5</sup> However, the dielectric permittivity of PDMS is relatively low ( $\sim 2.5$  at 1 kHz), which has greatly confined its application for high-performance DEG.<sup>6,7</sup> For this respect, two approaches were developed aiming at improving the dielectric permittivity of polymer composite in the past few years. One effective strategy is the addition of highly polarizable ceramic into the PDMS matrix such as barium titanate ( $\text{BaTiO}_3$ ),<sup>8,9</sup> titanium dioxide ( $\text{TiO}_2$ ),<sup>10</sup> and calcium copper titanate.<sup>11,12</sup> Despite the permittivity increase, the mechanical modulus of the PDMS-based composite would inevitably increase owing to the high loading content of the inorganic filler, which was unfavorable for DEG applications. To address this issue, the simultaneous incorporation of inorganic particles and plasticizer were also proposed, confirming the effectiveness of the method in reducing elastic modulus. For instance,  $\text{BaTiO}_3$  nanoparticles and dioctyl phthalate (DOP) plasticizer were simultaneously added into the natural rubber matrix by Zhang's group.<sup>13</sup> The as-prepared composite exhibited improved performances involving electric energy density ( $0.71 \text{ mJ cm}^{-3}$ ) and energy conversion efficiency (3.8%) comparing with pure natural rubber. Another commonly adopted approach to increase the dielectric permittivity is the incorporation of conductive fillers such as metallic particles and carbon nanomaterial.<sup>14–16</sup> Affording by the penetration effect, the metallic particles at low loading content enhanced the permittivity without significantly increasing the elastic modulus. Tian's group reported the fabrication of PDMS composite loaded with thermally expanded graphene nanoplates, which exhibited higher dielectric permittivity, lower dielectric loss, and larger actuated strain comparing with pure PDMS.<sup>17</sup> Unfortunately, the electromechanical transformation performances for the reported materials were still far from ideal resulting from the large disparity in dielectric permittivity and surface energy between the particle form filler and polymers. Therefore, the challenge of fabricating ideal dielectric materials lies in the synergistic implementation of high dielectric permittivity, low dielectric loss, and appropriate mechanical properties. A new type of push–pull dipole has been synthesized and grafted to the crosslinker molecules of the silicone rubber network by Guggi Kofod's group, which facilitated the homogenous elastomer composite of molecular level dispersion and resulted in relatively high permittivity and the low mechanical stiffness.<sup>18</sup> Besides, Anne Ladegaard Skov's group also used azobenzene dipoles as crosslinkers of the PDMS network and the dielectric constant of the resultant

composite was found to increase by 20% when the loading content of azobenzene was only 0.46 wt% while no significant change was observed for the mechanical properties.<sup>19</sup> These results further confirmed the great promise of chemically grafting strongly polar molecules onto the PDMS matrix for improved electromechanical transformation performance. However, the breakdown strength of the macromolecular network was reduced by nearly 70% at a high dipole graft ratio in Guggi Kofod's study. Furthermore, the energy harvesting performance of such dipole-modified matrix as DEGs has never been reported so far.

Herein, azobenzene molecules with high permanent dipole moments were synthesized and subsequently introduced into the crosslinked network to enhance the electrical generation performance. In addition, dimethyl silicone oil (DMSO) plasticizer was simultaneously added to reduce the mechanical modulus of the composite, offering the final composite denoting as *azo-g*-PDMS/DMSO. Through carefully optimizing the loading content of the strong polar molecules, the dielectric permittivity and the breakdown strength of the composite were simultaneously increased. Meanwhile, the as-prepared composites were tested in a conditioning circuit, evaluating their application as DEG. High energy harvesting density ( $0.69 \text{ mJ cm}^{-3}$ ), high electro-mechanical conversion efficiency (5.01%), and operating capability at high voltages were achieved for rubber composite containing 7 phr azobenzene dipoles because of its high dielectric permittivity and relatively low elastic modulus, highlighting its great potential for practical applications.

## 2. Experimental

### 2.1 Synthesis of azobenzene

The azobenzene chromophore was synthesized by an azo-coupling reaction according to the previous report.<sup>20</sup> Firstly, 4-nitroaniline (1.8 g) was dissolved in 30 mL of glacial acetic acid, followed by dropwise adding 4 mL of concentrated sulfuric acid. After stirred at  $0^\circ\text{C}$  for 5 min, 15 mL aqueous solution containing 1 g of sodium nitrite was added dropwise to the system, generating the brown-yellow diazonium salts. Secondly, the resulting diazonium salt solution was added dropwise to the solution of *N,N*-diethanolamine (2.0 g, in 250 mL of DMF), and the obtained mixture was reacted at  $0^\circ\text{C}$  for 12 h. After that, the reacted solution was mixed with deionized water in a ratio of 1 : 6. The insoluble precipitate was collected after filtration and washing with water and ethanol repeatedly. The azobenzene power was obtained after drying in the vacuum oven overnight at  $60^\circ\text{C}$ .

### 2.2 Preparation of *azo-g*-PDMS/DMSO

Hydroxyl-terminated polysiloxane precursors with two different molecular weights (long-chain: 90 000 mPa s, short-chain: 2000 mPa s) were employed to fabricate the silicone rubber matrix in the weight ratio of 80 : 20. Then, tetraethyl orthosilicate (TEOS), dibutyltin dilaurate, and dimethyl silicone oil (DMSO) were added as the crosslinker, catalyst, and plasticizer, respectively.



The rubber composites were prepared according to the formula and procedures previously reported.<sup>21</sup> Briefly, azobenzene power and TEOS were dissolved in tetrahydrofuran (THF) and stirred at 60 °C for 12 h. Then, PDMS (2.0 g), dibutyltin dilaurate (0.01 mL), and DMSO were added to the solution, followed by solvent evaporation at 60 °C for 2 h to completely remove the THF. Finally, the viscous mixture was transferred into a mold and vulcanized at room temperature for 8 h under a pressure of 15 MPa, offering the azo-*g*-PDMS/DMSO.

### 2.3 Characterization

The cross-sectional morphology of the azobenzene/silicone rubber composites was observed using scanning electron microscopy (SEM, Hitachi S-4800, Japan). The obtained azobenzene power was analyzed by Fourier transform infrared (FTIR) spectra (Nicolet, USA). Dielectric permittivity and loss tangent were measured using an impedance analyzer (Agilent 4294A) in the frequency range of 100–10 MHz at room temperature. The mechanical performances of the azo-*g*-PDMS/DMSO rubber composites were characterized using the universal mechanical testing machine (Shimadzu AG-IC, Japan). The rubber composites were immersed in silicone oil and the breakdown strength was tested using the high voltage amplifier (CS2674A) with a sphere-to-sphere electrodes configuration at the ramp rate of 200 V s<sup>-1</sup>. The energy harvesting performance of the azo-*g*-PDMS/DMSO films was evaluated according to the previous report using a set of instruments including oscilloscope, high voltage source, tensile machine, and a pair of circular clamps.<sup>22</sup>

## 3. Results and discussions

As mentioned above, the permittivity of polymers can be effectively improved through the introduction of functional groups with high permanent dipole moments into the chain structure. In this respect, the pseudo-stilbene type azobenzene with push-pull substituents, demonstrate a considerable dipole moment. Therefore, a typical pseudo-stilbene azobenzene with strong polarity was employed in this study, as shown in Scheme 1. Firstly, the synthesized azobenzene was analyzed with FTIR, as demonstrated in Fig. 1. The absorption peak at 3288 cm<sup>-1</sup> is the stretching vibration peak of the hydroxyl group, while the peaks at 1511 cm<sup>-1</sup> and 1344 cm<sup>-1</sup> belong to the symmetrical and asymmetrical absorption of the nitro group, respectively.

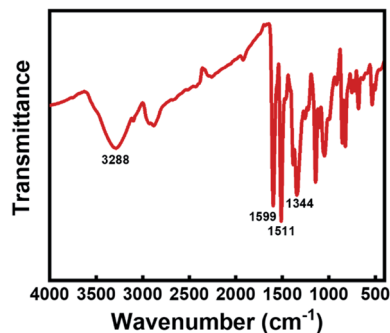
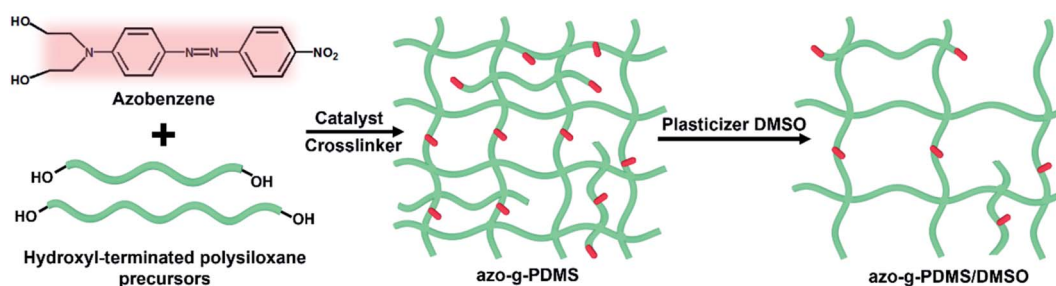


Fig. 1 The FTIR spectrum of synthesized azobenzene.

Particularly, the peak at 1599 cm<sup>-1</sup> refers to the characteristic absorption of the –N=N– group, confirming the formation of target azobenzene. The amino group is the electron donor while the nitro group is the electron acceptor, providing the dipole moment of 9 D for the pigment molecule.<sup>23</sup> Moreover, the azobenzene molecules are terminated with hydroxyl groups, which will compete with the terminal hydroxyl groups of the PDMS matrix during crosslinking, resulting in the random decoration of azobenzene onto the network. Though the grafting of azobenzene molecules is favorable for the homogeneous dispersion, the mechanical modulus and the mechanical energy required for stretching of the silicone rubber composite will be inevitably increased. Considering that, DMSO was further added as the plasticizer to reduce the mechanical stiffness of the azo-*g*-PDMS/DMSO films. However, the permittivity of DMSO is relatively low and its addition to the matrix will adversely affect the dielectric performance of the rubber composite. To balance these parameters, the loading content of the plasticizer was optimized in terms of the dielectric constant and mechanical modulus of the rubber matrix when 7 phr azobenzene was loaded. The elastic modulus of the pure PDMS matrix was about 0.34 MPa while it increased to 0.58 MPa in the case of azobenzene addition owing to the increased intermolecular interaction. As shown in Fig. 2, the elastic modulus of the rubber composite decreased significantly with the loading of DMSO, which was mainly attributed to weakened interactions between the macromolecular chains of PDMS and azobenzene molecules. Besides, the dielectric constant of the rubber composite slightly increased initially and then decreased with the increase of DMSO content. As a small



Scheme 1 The fabrication process of the azo-*g*-PDMS/DMSO.



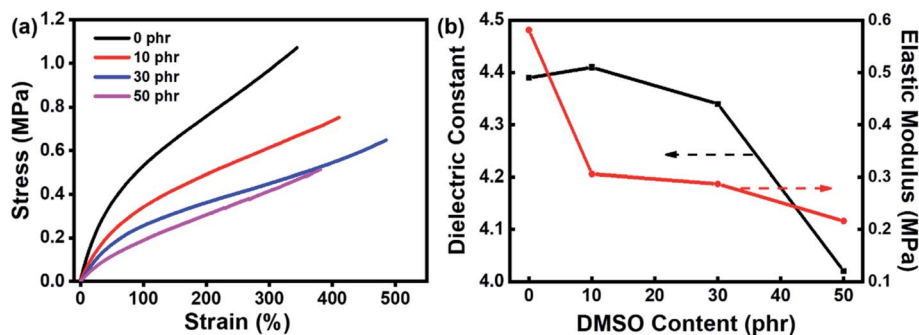


Fig. 2 The influence of DMSO content on (a) the tensile properties, (b) dielectric constant, and elastic modulus of bimodal PDMS grafted with 7 phr of azobenzene.

amount of DMSO was added, azobenzene molecules with strong polarity could get rid of the restriction between rubber molecular chains, leading to the enhanced polarization along the direction of the electric field. The increase of orientation polarization rate offsets the negative influence of plasticizer, resulting in a slight increase of the permittivity. However, when the DMSO content was greater than 10 phr, the dielectric constant of the azo-g-PDMS/DMSO film began to decrease owing to the relatively reduced content of the polar azobenzene molecules and the low dielectric constant of the plasticizer itself. For instance, the elastic modulus is reduced by 50% and the dielectric constant is reduced by 7% when 30 phr of DMSO was added. Overall, the optimal loading content of DMSO for subsequent preparation of rubber composite was rated as 30 phr.

Following the optimization of DMSO content, different amounts of azobenzene molecules were added to the matrix. The SEM images in Fig. 3 demonstrated the cross-sectional morphologies of the azo-g-PDMS/DMSO films loading with different amounts of polar azobenzene molecules. It can be seen that the addition of azobenzene molecules had no obvious influence on the morphology of the rubber composite even at

higher content, which greatly highlighted the superiority of molecular grafting azobenzene to the macromolecular network.

The stress-strain curves of the azo-g-PDMS/DMSO with different azobenzene contents were shown in Fig. 4. When small amounts of azobenzene molecules were grafted, the break elongation increased with the increase of dipoles loading content. As high as 570% of the elongation at break could be reached for the azo-g-PDMS/DMSO while 7 phr of azobenzene molecules were incorporated. When further adding azobenzene molecules to the matrix, the break elongation of azo-g-PDMS/DMSO starts to decline. In contrast, the tensile strength of the rubber composite displayed a continuously rising trend with the increase of azobenzene molecules content. On one hand, the introduced azobenzene molecules in the rubber composite can act as stress concentration to dissipate the loaded energy, thus contributing to better stress tolerance and higher break elongation. On the other hand, the excessive addition of azobenzene molecules can significantly increase the crosslinking density of the rubber composite, which restricted the movement of molecular chains and resulted in high elastic modulus and tensile strength. It should be further noted that the elastic modulus of the azo-g-PDMS/DMSO is comparable to pure

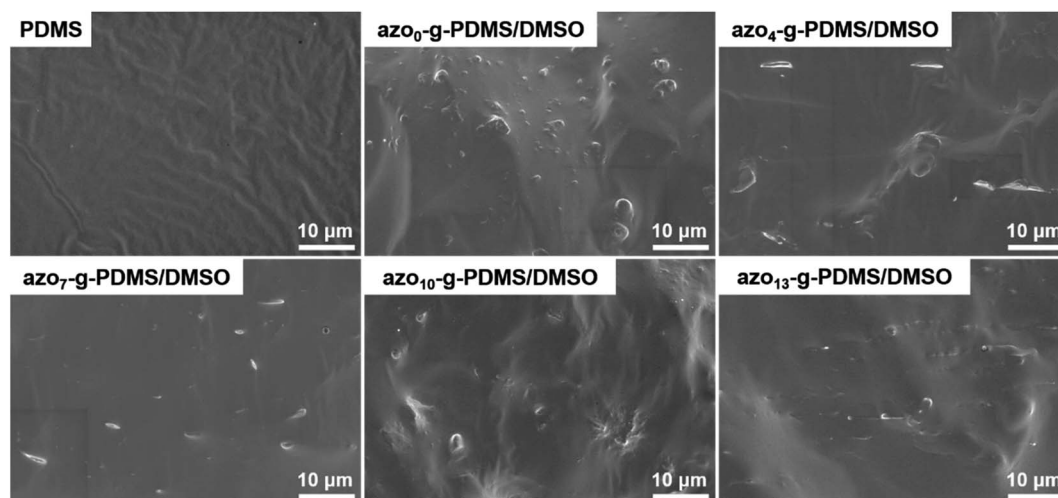


Fig. 3 Cross-sectional SEM images of the azo-g-PDMS/DMSO films incorporated with different mass contents of azobenzene molecules.



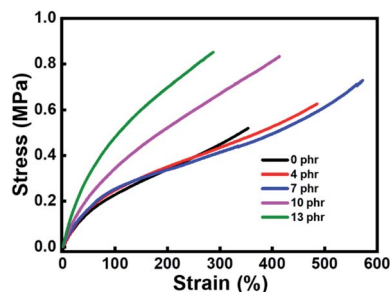


Fig. 4 Stress-strain curves of the azo-g-PDMS/DMSO films incorporated with different mass contents of azobenzene molecules.

silicone rubber matrix when the loading content of azobenzene is less than 7 phr, which was attributed to the plasticization effect of DMSO. Here, the introduction of azobenzene dipoles into the matrix resulted in the higher break elongation and unelevated elastic modulus, which provided favorable support for preparing elastomers with high electromechanical transformation performance.

As an organic molecule with strong polarity, the grafting of azobenzene onto the silicone rubber network will affect the polarity of the system and result in dielectric permittivity changes of the rubber composite. Fig. 5a showed the dielectric properties of the rubber composites incorporated with different amounts of azobenzene dipoles. When azobenzene content was low, the dielectric permittivity of the rubber composite at the same frequency was significantly increased with the increasing of azobenzene content, indicating the positive effect of azobenzene grafting. After grafted with a high level of azobenzene, the orientation polarization of grafted azobenzene under electric field will be greatly restricted because of the high cross-linking density, resulting in the slow increase of dielectric permittivity. The dielectric loss of the azo-g-PDMS/DMSO films with different azobenzene loading contents at the frequency of  $10^4$  Hz was present in Fig. 5b. Overall, the dielectric loss of the azo-g-PDMS/DMSO films increased with the increase of azobenzene contents. The orientation polarization of grafted azobenzene was restricted at higher loading, which increased the

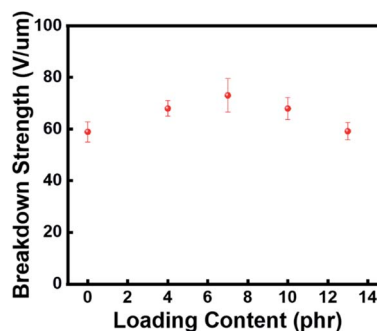


Fig. 6 Influences of azobenzene loading contents on the breakdown strength of the azo-g-PDMS/DMSO films.

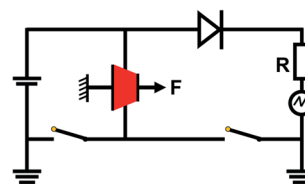


Fig. 7 The schematic illustration of the DEG operating circuit used to evaluate the electromechanical transformation performance of the azo-g-PDMS/DMSO films.

internal resistance need to be overcome, leading to higher dielectric loss. The breakdown strength of the rubber composite after azobenzene grafting was also evaluated, as shown in Fig. 6. Overall, the breakdown strength increased initially and then decreased with the increase of the azobenzene content. The breakdown strength of azo-g-PDMS/DMSO contains 7 phr of azobenzene can reach as high as  $73 \text{ V } \mu\text{m}^{-1}$ . This result was due to the introduction of azobenzene molecules partly repaired the defects of the silicone rubber matrix and suppressed the electric field distortion. Moreover, the free electrons would be trapped by the induced azobenzene, contributing to a higher breakdown strength.

Generally, the incorporation of azobenzene molecules significantly improved the mechanical and dielectric properties

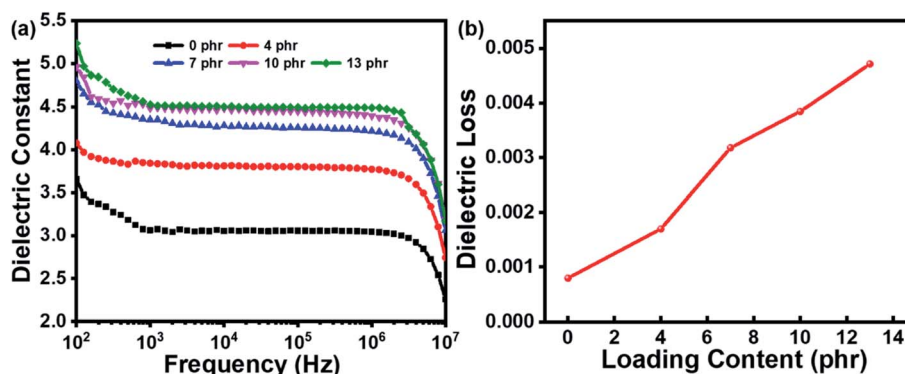


Fig. 5 The dielectric performance of the azo-g-PDMS/DMSO films. (a) Frequency dependence of dielectric constant for azo-g-PDMS/DMSO with different azobenzene loading contents; (b) influences of azobenzene loading contents on the dielectric loss of the azo-g-PDMS/DMSO films at the frequency of  $10^4$  Hz.



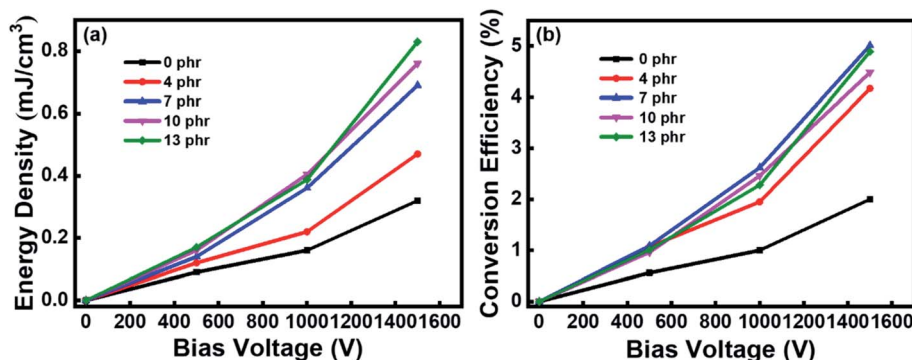


Fig. 8 (a) The volumetric energy density and (b) the mechano-electrical conversion efficiency of the azo-g-PDMS/DMSO with different azobenzene loading contents.

of the azo-g-PDMS/DMSO films, which provided favorable supports for their application as DEG. The electricity harvesting performance of the azo-g-PDMS/DMSO film was then evaluated according to the circuit demonstrated in Fig. 7. The test conditions were as same as those in the previous report.<sup>24</sup> The volumetric energy densities generated by the rubber composite under bias voltages of 500, 1000, and 1500 V were calculated, respectively. The material density of the azo-g-PDMS/DMSO was about  $0.975 \text{ g cm}^{-3}$ , so the generated electrical energy could also be expressed as mass energy densities as needed.<sup>25,26</sup> As demonstrated in Fig. 8a, higher electrical energy was generated for rubber composite with higher dielectric permittivity under the same bias voltage. Besides, the increase of generated electrical energy was slightly larger than the increase of bias voltage due to the increase of the electrode's resistance and relatively small voltage loss of the system. The energy density generated at 1500 V was about  $0.83 \text{ mJ cm}^{-3}$  when 13 phr azobenzene was grafted, which was about 2.5 times to the PDMS/DMSO matrix ( $0.32 \text{ mJ cm}^{-3}$ ). The mechano-electric energy conversion efficiency of the rubber composites grafting with different amounts of azobenzene was also calculated based on the electric and mechanical input, as demonstrated in Fig. 8b. The result

indicated that the electro-mechanical conversion efficiency increased with the increase of the bias voltage. The highest electromechanical conversion efficiency (5.01%) was achieved for rubber composite containing 7 phr azobenzene dipoles because of its high dielectric permittivity and relatively low elastic modulus.

The comparison of the dielectric property and energy harvesting abilities of this azo-g-PDMS/DMSO with reported literature were summarized in Table 1. Previous work by Kofod's group succeeded in simultaneously increasing the dielectric permittivity and reducing the elastic modulus in PDMS by synthesizing push-pull dipoles that were also grafted onto the crosslinker molecules of the silicone rubber.<sup>18</sup> However, the breakdown strength was also reduced by nearly 70% with dipole contents increasing from 0 wt% to 13.4 wt%. In addition, the energy harvesting performance of the as-prepared materials as DEG had not been demonstrated. Another group also reported the methyl-3-mercaptopropionate grafted poly(styrene-butadiene-styrene) (M3M-SBS) with higher dielectric permittivity (7.5) and energy harvesting density ( $9.57 \text{ mJ cm}^{-3}$ ), but the conversion efficiency was quite low (1.3%).<sup>27</sup> Other material systems based on BT/rubber were also confronted with the issue

Table 1 Comparison of dielectric properties and energy harvesting performance for the azo-g-PDMS/DMSO and the state-of-the-art in the literature

Materials	Dielectric permittivity (@1 kHz)	Maximum operating voltage (V)	Breakdown strength ( $\text{V } \mu\text{m}^{-1}$ )	DEGs application		Ref.
				Energy harvesting density ( $\text{mJ cm}^{-3}$ )	Conversion efficiency (%)	
Dipole grafted PDMS	5.98	—	39.0	—	—	18
Dipole grafted PDMS	3.30	—	91.9	—	—	19
M3M grafted SBS <sup>a</sup>	7.50	2000	39.6	9.57	1.3	27
BT/PU <sup>b</sup>	8.60	900	85	1.56	2.88	28
BT/plasticizer/PU	9.50	900	52.1	1.71	<1	22
BT/plasticizer/NR <sup>c</sup>	3.76	1400	40.3	0.71	3.8	13
CCTO/PDMS <sup>d</sup>	5.70	1500	55	0.69	3.02	24
Dipole grafted PDMS/plasticizer	4.35	1500	73	0.69	5.01	This work

<sup>a</sup> M3M: methyl-3-mercaptopropionate; SBS: poly(styrene-butadiene-styrene). <sup>b</sup> BT: barium titanate; PU: polyurethane. <sup>c</sup> NR: natural rubber. <sup>d</sup> CCTO: copper calcium titanate.

of low conversion efficiency. In general, the as-prepared rubber composite displayed considerable advantages over the previously reported rubber composite including high energy harvesting density ( $0.69 \text{ mJ cm}^{-3}$ ), high breakdown strength ( $73 \text{ V } \mu\text{m}^{-1}$ ), high electro-mechanical conversion efficiency (5.01%), and operating capability at high voltages.

## 4. Conclusions

In this work, strong polar azobenzene molecules were synthesized and covalently grafted onto the PDMS network to enhance its orientational polarization and energy harvesting performance. Furthermore, DMSO plasticizer was simultaneously added to reduce the mechanical modulus of the composite. The dielectric constant and the breakdown strength of the resultant azo-g-PDMS/DMSO films were simultaneously improved while keeping a relatively low level of mechanical stiffness. The maximum breakdown strength of the azo-g-PDMS/DMSO could reach  $73 \text{ V } \mu\text{m}^{-1}$  with 7 phr azobenzene. In addition, the as-prepared rubber composite displayed high energy harvesting density ( $0.69 \text{ mJ cm}^{-3}$ ) and high electro-mechanical conversion efficiency (5.01%) at a bias voltage of 1500 V, which were 2 and 2.5 times as much as the azobenzene-free matrix, respectively. These results show that it is possible to achieve superior energy harvesting performance for DEG applications by grafting azobenzene with high dipole moments to the macromolecular network.

## Conflicts of interest

There are no conflicts of interest to declare.

## Acknowledgements

This work was financially supported by the China Postdoctoral Science Foundation (2019M660457), the 1226 Engineering Health Key Project (BWS17J028), the Fundamental Research Funds for the Central Universities (FRF-TP-19-058A1), and the Interdisciplinary Research Project for Young Teachers of USTB (FRF-IDRY-19-003).

## References

- 1 G. Moretti, S. Rosset, R. Vertechy, I. Anderson and M. Fontana, *Adv. Intell. Syst.*, 2020, **2**, 2000125.
- 2 D. M. Opris, M. Molberg, C. Walder, Y. S. Ko, B. Fischer and F. A. Nüesch, *Adv. Funct. Mater.*, 2011, **21**, 3531–3539.
- 3 F. Carpi, I. Anderson, S. Bauer, G. Frediani, G. Gallone, M. Gei, C. Graaf, C. Jean-Mistral, W. Kaal, G. Kofod, M. Kollosche, R. Kornbluh, B. Lassen, M. Matysek, S. Michel, S. Nowak, B. O'Brien, Q. Pei, R. Pelrine, B. Rechenbach, S. Rosset and H. Shea, *Smart Mater. Struct.*, 2015, **24**, 105025.
- 4 B. Fasolt, M. Hodgins, G. Rizzello and S. Seelecke, *Sens. Actuators, A*, 2017, **265**, 10–19.
- 5 M. P. Wolf, G. B. Salieb-Beugelaar and P. Hunziker, *Prog. Polym. Sci.*, 2018, **83**, 97–134.
- 6 H. Sun, X. Liu, B. Yu, Z. Feng, N. Ning, G.-H. Hu, M. Tian and L. Zhang, *Polym. Chem.*, 2019, **10**, 633–645.
- 7 L. Duan, J. Zhang, M. Zhang, C.-H. Li and J.-L. Zuo, *J. Mater. Chem. C*, 2018, **6**, 12175–12179.
- 8 H. Zhao, L. Zhang, M.-H. Yang, Z.-M. Dang and J. Bai, *Appl. Phys. Lett.*, 2015, **106**, 092904.
- 9 D. Yang, S. Huang, M. Ruan, S. Li, Y. Wu, W. Guo and L. Zhang, *Compos. Sci. Technol.*, 2018, **155**, 160–168.
- 10 H. Liu, L. Zhang, D. Yang, Y. Yu, L. Yao and M. Tian, *Soft Mater.*, 2013, **11**, 363–370.
- 11 Y. Y. Zhang, G. L. Wang, J. Zhang, K. H. Ding, Z. F. Wang and M. Zhang, *Polym. Compos.*, 2019, **40**, E62–E68.
- 12 G. L. Wang, Y. Y. Zhang, L. Duan, K. H. Ding, Z. F. Wang and M. Zhang, *J. Appl. Polym. Sci.*, 2015, **132**, 42613.
- 13 D. Yang, Y. Xu, M. Ruan, Z. Xiao, W. Guo, H. Wang and L. Zhang, *AIP Adv.*, 2019, **9**, 025035.
- 14 Z. Xu, S. Zheng, X. Wu, Z. Liu, R. Bao, W. Yang and M. Yang, *Composites, Part A*, 2019, **125**, 105527.
- 15 J. Biggs, K. Danielmeier, J. Hitzbleck, J. Krause, T. Kridl, S. Nowak, E. Orselli, X. Quan, D. Schapeler, W. Sutherland and J. Wagner, *Angew. Chem., Int. Ed.*, 2013, **52**, 9409–9421.
- 16 M. Panahi-Sarmad, E. Chehraz, M. Noroozi, M. Raef, M. Razzaghi-Kashani and M. A. H. Baian, *ACS Appl. Electron. Mater.*, 2019, **1**, 198–209.
- 17 M. Tian, Z. Wei, X. Zan, L. Zhang, J. Zhang, Q. Ma, N. Ning and T. Nishi, *Compos. Sci. Technol.*, 2014, **99**, 37–44.
- 18 B. Kussmaul, S. Risse, G. Kofod, R. Waché, M. Wegener, D. N. McCarthy, H. Krüger and R. Gerhard, *Adv. Funct. Mater.*, 2011, **21**, 4589–4594.
- 19 F. B. Madsen, A. E. Daugaard, S. Hvilsted, M. Y. Benslimane and A. L. Skov, *Smart Mater. Struct.*, 2013, **22**, 104002.
- 20 P. C. Che, Y. N. He and X. G. Wang, *Macromolecules*, 2005, **38**, 8657–8663.
- 21 L. Zhang, D. Wang, P. Hu, J.-W. Zha, F. You, S.-T. Li and Z.-M. Dang, *J. Mater. Chem. C*, 2015, **3**, 4883–4889.
- 22 G. Yin, Y. Yang, F. Song, C. Renard, Z. M. Dang, C. Y. Shi and D. Wang, *ACS Appl. Mater. Interfaces*, 2017, **9**, 5237–5243.
- 23 J. M. Simmons, I. In, V. E. Campbell, T. J. Mark, F. Leonard, P. Gopalan and M. A. Eriksson, *Phys. Rev. Lett.*, 2007, **98**, 086802.
- 24 L. Zhang, F. Song, X. Lin and D. Wang, *Mater. Chem. Phys.*, 2020, **241**, 122373.
- 25 S. J. A. Koh, C. Keplinger, T. Li, S. Bauer and Z. Suo, *IEEE ASME Trans. Mechatron.*, 2011, **16**, 33–41.
- 26 T. G. McKay, B. M. O'Brien, E. P. Calius and I. A. Anderson, *Appl. Phys. Lett.*, 2011, **98**, 142903.
- 27 C. Ellingford, R. Zhang, A. M. Wemyss, Y. Zhang, O. B. Brown, H. Zhou, P. Keogh, C. Bowen and C. Wan, *ACS Appl. Mater. Interfaces*, 2020, **12**, 7595–7604.
- 28 Y. Yang, Z.-S. Gao, M. Yang, M.-S. Zheng, D.-R. Wang, J.-W. Zha, Y.-Q. Wen and Z.-M. Dang, *Nano Energy*, 2019, **59**, 363–371.

